Alzheimer's
Research & Therapy

RESEARCH

Open Access

Protein co-aggregates of dense core amyloid plaques and CSF differ in rapidly progressive Alzheimer's disease and slower sporadic Alzheimer's disease

Gurkan Bebek[1], Masaru Miyagi[2], Xinglong Wang[3], Brian S. Appleby[4], James B. Leverenz[5] and Jagan A. Pillai[5*]

Abstract

Background The rapidly progressive phenotype of Alzheimer's disease (rpAD) remains a rare and less-studied entity. Therefore, the replication of key results from the rpAD brain and cerebrospinal fluid (CSF) is lacking.

Methods A label-free quantitative LC-MS/MS analysis of proteins co-aggregating with core-amyloidβ plaques in fresh frozen tissue (FFT) from medial temporal regions of rpAD ($n = 8$) neuropathologically characterized at the National Prion Disease Pathology Surveillance Center (NPDPSC), compared with microdissected amyloid plaques from formalin-fixed, paraffin-embedded (FFPE) tissue blocks from patients with rpAD ($n = 22$) previously published from the NPDPSC cohort, was performed. Matched rpAD CSF from the FFT cases were compared to a previously published proteomic evaluation of CSF in the AD subtype with rapid progression.

Results A total of 1841 proteins were characterized in the FFT study, of which 463 were consistently identified in every rpAD patient analyzed. One thousand two hundred eighty-three proteins were shared between the FFT and the prior FFPE study. FFT offered a more comprehensive proteomic profile than the prior FFPE study and prominently included the immune system pathways. Thirty-five proteins were shared in the FFT brain tissue, matched CSF from the same subjects, in which biological processes related to immune response were again notable. These results were validated against prior published proteomic CSF AD data with a faster rate of progression to identify the top 5 potential protein biomarkers of rapid progression in AD CSF.

Conclusions These results support a distinct immune-related proteomic profile in both the brain and the CSF that can be explored as potential biomarkers in the future for the clinical diagnosis of rpAD.

Keywords Rapidly progressive Alzheimer's disease, Proteomics, Cerebrospinal fluid, Fresh frozen tissue, Formalin-fixed, Paraffin-embedded tissue, Dense core amyloid plaque, Neuroinflammation, Alzheimer's disease, Dementia, Rapidly progressive dementia, Proteomics, Dense core amyloid plaque, Autopsy, CSF

*Correspondence:
Jagan A. Pillai
pillaij@ccf.org
Full list of author information is available at the end of the article

Introduction

Alzheimer's Disease (AD) is among the defining public health concerns of the 21 st century and is now a leading cause of disability worldwide [1, 2]. Although AD is classically described by neuropathological changes in amyloidβ plaques and tau neurofibrillary tangles in the brain [3], (Alzheimer's Disease Neuropathologic Change, ADNC), there is substantial clinical heterogeneity among patients with AD [4, 5]. The trajectory of clinical decline among AD patients can vary widely from less than 1 year to over 10 years [6]. This heterogeneity, particularly in the rate of clinical decline, entails a huge challenge in evaluating patients and developing a new generation of therapies [7–9]. Factors such as age, sex, genetics, socioeconomic status, medical comorbidity, and cognitive reserve are thought to affect the rate of AD clinical progression [10].

A rapidly progressive subtype of AD (rpAD), among autopsy-confirmed cases with a survival duration of less than 3 years has been reported by us in two US national cohorts, the National Prion Disease Pathology Surveillance Center (NPDPSC) and the National Alzheimer's Coordinating Center (NACC), despite different recruitment biases [9]. In prion disease surveillance centers worldwide, AD is the most frequent diagnosis of non-prion disease at autopsy, accounting for 14 to 50% of all non-prion cases, since rpAD is associated with a diversity of neurological signs and can mimic Creutzfeldt-Jakob disease [11, 12]. Here, the rpAD phenotype has been well established as detailed clinical data supporting a rapid disease course is available [6, 11, 13]. Several studies have noted differences in the allelic frequency of APOE $\epsilon 4$, structural organization of the Aβ species, tau seeding, and amyloid plaque composition between rpAD and slower progressing sporadic AD (spAD) [6, 11–17]. Together they support the view that rpAD represents an AD subtype with distinct biological characteristics.

Despite increasing interest in rpAD, most studies have included a modest number of rpAD cases, typically fewer than 30. This is likely due to its rarity and the challenges of accurate characterization via disease biomarkers in rapid progression. When establishing clinical biomarker evaluation or therapeutic targets among cases of rpAD, these studies are consequently limited by the relatively small number of well-characterized rpAD cases. Furthermore, ensuring consistent results across different cohorts and within the same cohort is crucial, especially when varied sample preparation methods are likely to influence the outcomes. This is also true in the context of proteomic evaluation of amyloid core plaques, which represent one of the central neuropathological hallmarks of AD among rpAD cases.

Our study was driven by the overarching goal of advancing our comprehension of the biological signature in rpAD by seeing how replicable proteomic results across different analysis techniques are and if there is a shared proteomic signature between the brain and cerebrospinal fluid (CSF) of interest to develop as potential biomarkers. Our primary objective was the examination of proteins co-aggregating with dense core-amyloid plaques in fresh frozen tissue (FFT) samples from the medial temporal lobe in both phenotypes using mass spectrometry techniques. We hypothesized that a similar range of amyloid core plaque-related proteins from rpAD and spAD would be seen in both FFT tissue and the previously published formalin-fixed paraffin-embedded (FFPE) preparation techniques [15]. Furthermore, we explored whether there were overlapping proteins between the rpAD amyloid core plaques and CSF from these same cases.

Methods

Ethics statement

All procedures were performed under protocols approved by the Institutional Review Board at Case Western Reserve University. All patients' data and samples were coded and handled according to NIH guidelines to protect patients' identities.

National prion disease pathology surveillance center rpAD cohort

The rpAD cohort from the NPDPSC has been previously described [6, 13]. In brief, following the standard NPDPSC protocol, case records were retrospectively analyzed by trained personnel for the time of onset of symptoms noted by the physician and/or obtained from caregivers via standardized consent forms. As there are no consistent clinical criteria for rpAD, patients in the rpAD cohort met the following inclusion criteria: (i) suspected cases of prion disease referred to the NPDPSC; (ii) death within 3 years of initial symptoms; (iii) exclusion of prion disease via histology, immunohistochemistry, and western blot analyses; (iv) neuropathology and immunohistochemistry of tau proteins and amyloidβ with unequivocal classification as Alzheimer's disease according to the published guidelines [18]; (v) absence of neuropathologic comorbidity contributing to phenotype; (vi) absence of medical comorbidities that could affect disease progression (e.g., renal failure). Eight rpAD cases were included in the analysis, demographic details are provided in Table 1. These rpAD patient brains using FFT had the same sex distribution and range of disease duration as prior published reports using FFPE [15].

Slower progressing sporadic AD (spAD) cohort

AD patients with predominant amnestic symptoms from the Case Western Reserve University (CWRU) Memory

Table 1 Subject demographics

Diagnosis	Sex	Age at symptom onset (years)	Age at death (years)	Estimated symptom duration (years)
rpAD	Male	84	85	1
rpAD	Female	81	82	2
rpAD	Male	88	89	1
rpAD	Male	75	76	1
rpAD	Male	59	60	1
rpAD	Female	59	62	3
rpAD	Female	80	80	< 1
rpAD	Female	73	74	1
spAD	Male	NA	67	> 3
spAD	Female	NA	83	> 3
spAD	Female	NA	78	> 3

and Aging Center brain bank were used to constitute the spAD cohort. They met AD neuropathological evaluation criteria according to published guidelines [18]. Due to unavailable symptom onset data, 3 spAD cases with amnestic symptoms were randomly selected for estimated symptom duration from clinical records that noted clinical history over 3 years. This smaller sample size was used for exploratory analysis based on the variance between brains observed in a prior published report [15].

Individual-level data on Braak stage and Thal phase were not available for all subjects for detailed analysis. Inclusion of these data will be essential for future studies to enable more precise stratification and interpretation.

Demographic details are provided in Table 1.

Materials

Protease inhibitor cocktail and High Select™ Top14 Abundant Protein Depletion Mini Spin columns were purchased from Thermo Fisher Scientific (Waltham, MA). Lys-C was obtained from FUJIFILM Wako Chemicals U.S.A. (Richmond, VA). All other chemicals were either reagent grade or of the highest commercially available quality.

Amyloid core-plaque isolation and preparation

Compared with the previous study using laser-capture microdissection (LCM) to isolate plaques or regions within plaques [15], this study focused on studying the properties and molecular composition at the center of the plaques. Amyloid plaque cores were isolated as previously described [19]. Briefly, human brain gray matter were homogenized in lysis buffer (2% SDS, 50 mM Tris-HCl pH 7.5, 50 mM DTT, 1x protease inhibitor cocktail) using a Dounce glass homogenizer, boiled for 10 min, and centrifuged at 100 000×g for 1 h at 10°C. Then, the pellet was solubilized in fraction buffer (1% SDS, 50 mM Tris-HCl pH 7.5, 50 mM DTT) and centrifuged at 100 000×g for 1 h at 10°C. The resulting pellet was suspended in a fraction buffer and loaded on top of a discontinuous sucrose gradient (1.0, 1.2, 1.4, and 2.0M sucrose in 50 mM Tris pH 7.5 containing 1% SDS), centrifuged at 220 000×g for 20 h at 10°C, and the interface region between 1.4 and 2.0M sucrose was collected. The plaque-core-enriched fraction was resuspended in water and centrifuged at 100 000×g for 1 h at 4°C. The resulting pellet was dissolved in urea buffer (7 M urea, 2 M thiourea, 4% CHAPS, 30 mM Tris, 5 mM magnesium acetate, pH 8.5, 1× protease inhibitor cocktail, 1× phosphatase inhibitor cocktail), centrifuged at 18 000×g for 30 min, and the supernatants were collected. The protein concentration was estimated with a Bradford assay.

Cerebrospinal fluid (CSF) samples

CSF from patients was obtained before death during their clinical diagnostic workup to rule out the existence of prion disease in rpAD cases.

Per the NPDPSC protocol, 2 mL of CSF (1 mL minimum), avoiding a bloody tap, was recommended to be collected in a polypropylene, low-binding, sterile collection tube. The samples were immediately frozen, at least in a −20°C freezer, and shipped to the NPDPSC on dry ice. Samples were stored in a −80°C freezer at NPDPSC after the initial analysis for prion disease, which was ruled out using RT-QuIC for prion proteins. AD diagnosis was confirmed at autopsy.

Proteomic analysis

The isolated amyloid plaque 10 µg was subjected to SDS-PAGE approximately ~1 cm into a 4–20% Mini-PROTEAN® TGX™ precast protein gel (Bio-Rad, Hercules, CA). The top 1 cm of the gel was then excised and in-gel digested by Lys-C [20]. A 50 µL sample of CSF was mixed directly with 1 µL of 10× protease inhibitor cocktail, and the most abundant 14 proteins were removed using a High Select™ Top14 Abundant Protein Depletion Mini Spin column according to the manufacturer's instructions. The resulting CSF was concentrated to approximately 100 µL using a 3 kDa molecular weight cut-off Amicon centrifuge filter unit (Millipore Sigma, Burlington, MA) and dried in a SpeedVac concentrator. The dried CSF was then subjected to SDS-PAGE and in-gel digested with Lys-C as described above. Following digestion, LC-MS/MS was performed using the Fusion Lumos™ Orbitrap Mass Spectrometer (Thermo Fisher Scientific). HPLC was carried out using a Dionex 15 cm × 75 µm id Acclaim Pepmap C18, 2 µm, 100Å reversed-phase capillary

chromatography column. Peptides eluted from the column in an acetonitrile/0.1% formic acid gradient (flow rate = 0.3 μL) were introduced into the microelectrospray ion source of the mass spectrometer, which was operated at 2.5 kV. Samples were analyzed using a data-dependent method with CID fragmentation. Proteins were identified by comparing all experimental peptide MS/MS spectra against the UniProt human database using the Andromeda search engine integrated into the MaxQuant version 1.6.3.3 [21, 22]. Carbamidomethylation of cysteine was set as a fixed modification, whereas variable modifications included oxidation of methionine to methionine sulfoxide and acetylation of N-terminal amino groups. For peptide/protein identification, strict Lys-C specificity was applied, the minimum peptide length was set to 7, the maximum missed cleavage was set to 2, and the cutoff false discovery rate was set to 0.01. Match between runs (match time window: 0.7 min; alignment time window: 20 min) and label-free quantitation (LFQ) options were enabled. The LFQ minimum ratio count was set to 2. The remaining parameters were kept as default. Protein quantitation was accomplished using Perseus [23]. LFQ values were log2-transformed, and missing values were imputed using the "Replace missing value from normal distribution" function on the entire matrix using default parameters (Please refer to Additional Files 2 and 3 for the data generated from amyloid plaque cores and CSF, respectively).

Bioinformatics analysis

A log transformation was initially applied to the protein-level identifications to reduce systematic variations in recorded intensities. Additionally, in line with our assumption of homoscedasticity within this multi-group design, we employed a joint adaptive mean-variance regularization procedure using the R package `MVR` [24]. This approach not only tackles the challenge posed by the $n \gg m$ problem, where the number of observations (n) significantly exceeds the number of variables (m), potentially resulting in statistical complexities and overfitting but also addresses the common issue of variance-mean dependence often encountered in expansive omics datasets.

Public data access

FFPE [15] and CSF [25] proteomics data were downloaded from the corresponding articles' supplementary data. In this study, we utilized protein identifications from these studies as the authors reported them. The signaling pathway database was downloaded from Reactome Database [26].

Differential expression analysis

Pairwise differentially expressed proteins were identified using ROTS [27], followed by Benjamini-Hochberg (BH) FDR correction. Differential expression was presented in volcano plots and heatmaps, generated with the `ggplot2` package in R.

GO and pathway enrichment analyses

To characterize proteins based on the GO annotation, we employed the `clusterProfiler` R package. The pruned output of Fisher's exact test was utilized for over-representation analysis, and the resulting z-scores were visualized through a custom R script. The background proteome comprised all proteins within each specific dataset. As previously outlined, enrichment analysis for each module was conducted by cross-referencing the respective gene symbols with sample gene lists. The significance of enrichment within each dataset was determined using a one-tailed Fisher's exact test and corrected for multiple comparisons using the Benjamini-Hochberg (BH) false discovery rate (FDR) method.

For the analysis of Reactome pathway databases, we utilized Over-Representation Analysis (ORA). The pathway database was queried at various levels of granularity by pruning the pathway tree at incremental depths in terms of pathway hierarchy. For instance, level 2 (L2) represented major pathways and their respective sub-pathways. We calculated one-tailed Fisher's exact tests and adjusted p-values using the BH method. The enrichment plots were generated using in-house scripts to visualize the comparison of enrichment in two datasets.

Principal component analysis of shared proteins

Principal component analysis (PCA) was conducted to identify major axes of variation within the proteomic data. We focused on the first principal component (PC1) as a potential marker of disease-related proteomic alterations. Spearman's rank correlation coefficients were calculated to assess the associations between PC1 and the expression levels of microtubule-associated protein tau (MAPT) and neurofilament light chain (NEFL), proteins commonly associated with tau pathology and axonal injury, respectively.

Results

Proteomic analysis and differential expression in rpAD and spAD patients

rpAD patients had a comparable mean age in years at autopsy to spAD patients [76.0 (SD 10.4) vs 76.0 (SD 8.2)]. Four of 8 rpAD cases were female, while 2 of 3

spAD cases were female. The nature and the distribution, count, and morphology of amyloid plaques were not uniquely evaluated for each of the brains. Subject demographics are noted in Table 1.

The dataset contained 1841 proteins, with 199 shared across both phenotypes and 463 unique to rpAD samples. Data imputation was used to address missing values, enhancing the reliability of protein expression profiles and improving the accuracy of subsequent analyses.

Differential expression analysis was conducted on the dataset normalized using the Systematic Variation Normalization (SVN) method, employing the Reproducibility Optimized Test Statistic (ROTS) [27], which identified proteins with significantly altered abundance levels (adj-p-value < 0.05) between spAD and rpAD cases (Supplementary Table S1). A total of 243 were significantly differentially altered, with 160 proteins showing decreased abundance and 83 proteins showing increased abundance in rpAD compared to spAD. In this comparison, we identified key AD-related genes, such as microtubule-associated protein tau (MAPT), beta-synuclein (SNCB), and clusterin (CLU) adj-p-value < 0.05) (Fig. 1A and B) [28–31]. Among the expressed genes, MAPT and amyloid-beta precursor protein (APP) levels were strongly correlated with the rpAD disease phenotype. As shown in Fig. 2A and B, unsupervised cluster analysis of MAPT and APP correlated protein expression grouped samples by disease phenotypes, rpAD and spAD.

Functional analysis of proteomic changes between the rpAD and spAD groups

Gene ontology (GO) analysis of the 243 significantly altered proteins revealed strong links to DNA Double-Strand Breaks (DSBs), Epigenetic Alterations, Thyroid Dysfunction, and Telomere Attrition (Supplementary Fig. S2 and Supplementary Table S2). Based on the annotation terms and shared genes, we can group significant terms into 3 essential functional groups: 1. Gene Silencing and Epigenetic Regulation, 2. DNA Repair and Telomere Organization, 3. Metabolic Processes and RNA Regulation (Fig. 3). These 3 groups show significant candidate pathway differences worthy of exploration in rpAD compared to spAD in future studies.

FFT vs FFPE comparison

A total of 1841 proteins were characterized in the current FFT study, of which 1283 proteins were shared between the current FFT and the prior FFPE study (Supplementary Fig. S1a). There were only 14 proteins that were significantly differentially expressed in both studies. The small overlap shows that the results of the two studies could likely vary based on the tissue preparation method and suggest variability in protein preservation in the different methods or samples used. To further understand the differences, we investigated the ontologies and pathways related to significantly altered proteins in both studies (Fig. 4). While we observe some overlap, the FFT dataset identified more pathways. The pathways identified are categorized into various biological processes (at top-level categories in the Reactome pathway database), including vesicle-mediated transport, signal transduction, sensory perception, programmed cell death, organelle biogenesis and maintenance, neuronal system, muscle contraction, metabolism of RNA and proteins, immune system, gene expression, disease, developmental biology, cellular responses to stimuli, cell-cell communication, and cell cycle.

Identifying a larger number of differentially expressed proteins and associated pathways in FFT compared to FFPE suggests that FFT preserves a broader range of protein co-aggregates, potentially offering a more comprehensive, albeit complex, molecular snapshot of the plaque environment, rather than necessarily a clearer distinction in all aspects (Supplementary Fig. S5).

Similarly, the gene ontology enrichment comparison between FFT and FFPE samples reveals that FFT samples offer more granular functional annotations and a more transparent disease comparison (rpAD vs spAD) (Supplementary Fig. S6).

rpAD FFT samples with matched CSF

We next evaluated CSF from rpAD cases with matched FFT brain tissue and compared the proteomic differences against a previously published CSF proteomic evaluation in AD subtypes identified by data-driven clustering methods on CSF proteins and controls [25]. Supplementary Fig. S7 A depicts the intersection of gene clusters enriched in both studies and those unique to each (120 for rpAD CSF only, 874 for CSF of Tijms et al. [25] and 435 shared across). We further investigated the enriched biological processes within these gene clusters, highlighting the functional differences between the two sample groups. Supplementary Fig. S7B shows a dot plot comparing gene enrichment between three groups: genes shared by both CSF and Tijms et al. [25] datasets, and genes unique to each study are shown. Both datasets share enrichment in biological processes like complement activation, humoral immune response, and extracellular matrix organization, indicating a common biological theme.

Additionally, we compared the rpAD amyloid plaque-related proteins from FFT samples to those of matched CSF samples and a CSF proteomic AD subtype with rapid progression identified in Tijms et al. [25] (Fig. 5). 35 proteins were identified across all three groups Fig. S8). GO enrichment analysis of these proteins showed that

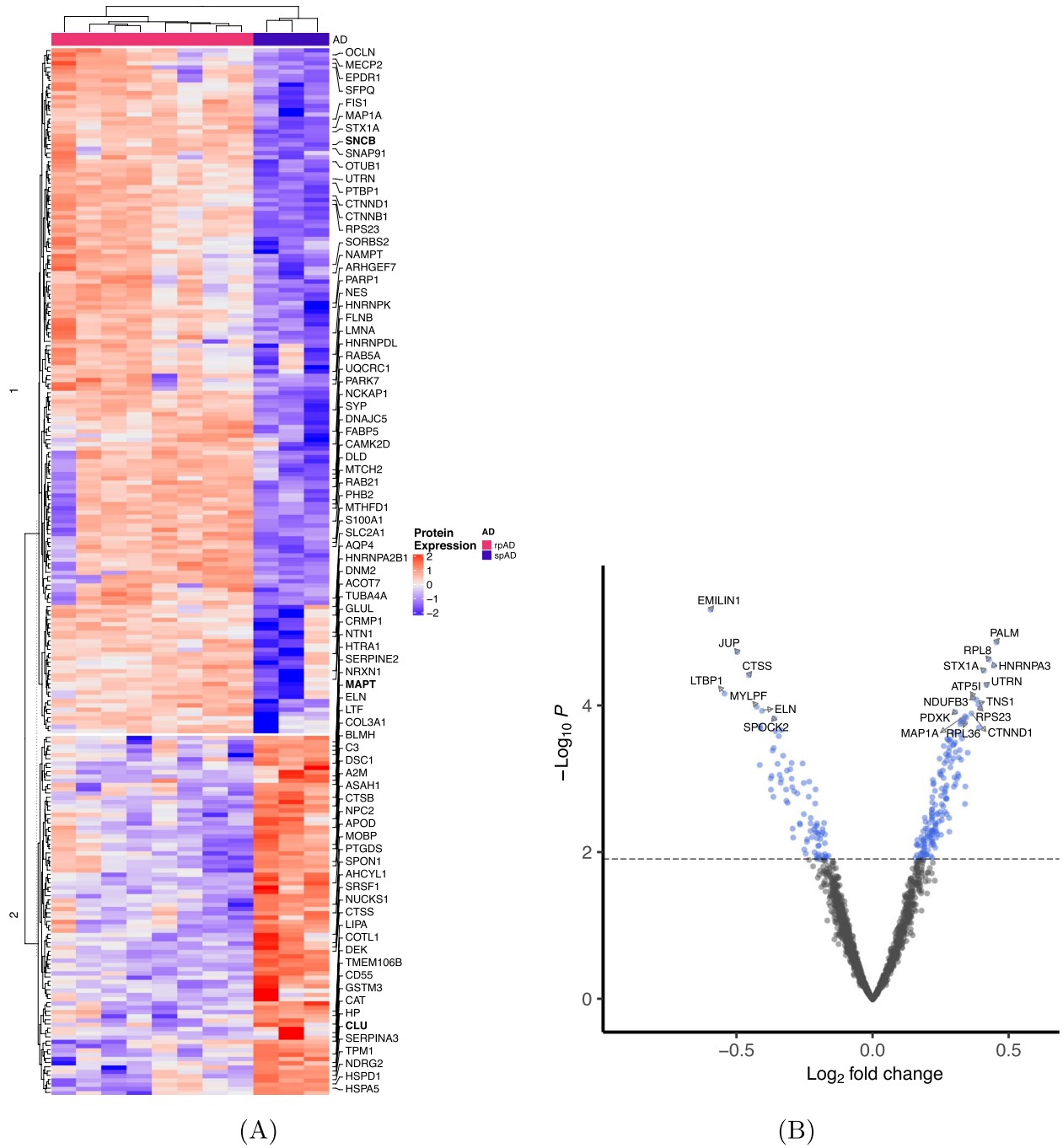

Fig. 1 **A** Heatmap of differentially expressed proteins and their association with AD. Heatmap of differentially expressed proteins (adj-p-value < 0.05). Genes known to be associated with AD are labeled on the right. The red color indicates increased expression. The top color bar labels rpAD (orange) and spAD (cyan) samples. **B** Volcano plot showing the differential expression of proteins between conditions. Volcano plot showing significantly different expression of proteins. Blue circles highlight proteins with statistically significant expression differences (adj-p-value < 0.05). Increased expression in rpAD is shown on the right

they are enriched in biological processes related to the immune response, including defense response, humoral immune response, complement activation, and acute inflammatory response (adj-p-value < 0.05).

Among the 35 genes, five genes—PGAM1, YWHAG, DLD, PARK7, and EPDR1—were upregulated, while the remaining 30 were downregulated (Fig. S8). Functional annotation demonstrated that the upregulated genes

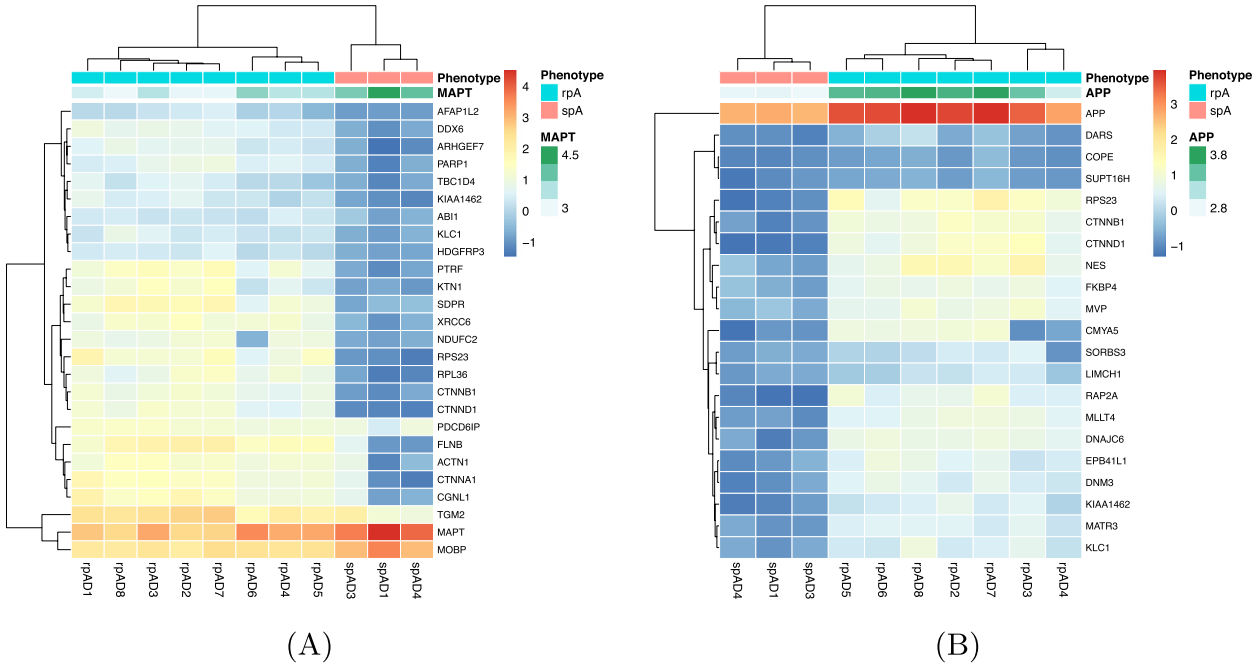

Fig. 2 Protein expression profiles of (**A**) MAPT-correlated and (**B**) APP-correlated proteins are shown. Pearson's correlation is calculated based on all sample profiles, and in these figures, any proteins that have an absolute correlation greater than 0.85 are shown (See Supplementary Fig. S1 for a lower threshold). The proteins are then subjected to unsupervised clustering. rpAD (rpA) and spAD (spA) samples separate based on their expression profiles

are mainly involved in glycolysis (PGAM1), mitochondrial metabolism (DLD), redox regulation (PARK7), stress signaling (YWHAG), and potential lysosomal and adhesion-related roles (EPDR1) [32–34]. In contrast, the downregulated set includes proteins critical to proteostasis (CLU, HSPA5), synaptic adhesion (NRXN1), complement regulation (C3, CD55), antioxidant defense (APOD, HP, GGCT), and extracellular matrix stability (LAMB1, NID2, FBLN1, SPON1) [34–39].

Pathway enrichment analysis based on these proteins underscores a widespread failure in multiple protective systems. There is downregulation in the complement cascade (C3, CD55), ER stress responses (HSPA5), lysosomal function (CTSB, CTSS, NPC2), Aβ modulation (CLU, SPON1, A2M), and ECM organization (LAMB1, NID2) [38–40]. Notably, synaptic structural proteins (NRXN1, TPM1) are reduced, suggesting rapid loss of neuronal connectivity [41].

Cathepsin S (CTSS) is a lysosomal cysteine protease that plays a key role in antigen presentation (via MHC class II pathway), proteolysis of extracellular matrix proteins, and microglial activation. The downregulation of CTSS in rpAD—contrasting its established upregulation in typical AD—suggests a distinct neuroinflammatory and proteostatic state is likely from early versus late stage of AD-dependent expression levels. This possibility of differential expression by AD stage is also seen with other CSF inflammatory proteins [42, 43]. In late-stage AD, compared to early-AD, microglia may shift from a pro-inflammatory to a dystrophic or exhausted state, leading to reduced CTSS expression. In spAD models, CTSS drives microglial M1 activation via the CX3 CL1-CX3 CR1-JAK2/STAT3 axis [44], and pharmacologic CTSS inhibition enhances BDNF/TrkB-mediated synaptic plasticity and cognitive performance in mice [45]. Its reduction in rpAD may reflect either a "burned-out" inflammatory response or loss of CTSS-expressing cell populations.

In parallel, YWHAG, a 14-3-3 protein, exacerbates tau pathology in AD by promoting tau hyperphosphorylation through its interaction with tau and tau-phosphorylating kinases [46]. It also stabilizes hyperphosphorylated tau, preventing its degradation and contributing to toxic aggregate accumulation and neuronal dysfunction [46]. Additionally, YWHAG upregulation disrupts protein homeostasis and promotes calcium dysregulation and ER stress via pathways like C/EBPβ-TRPC1-SOCE, further aggravating tau aggregation and neurodegeneration [47].

The downregulation of GGCT, TPM1, and SPON1 points to synergistic vulnerabilities. GGCT's role in glutathione metabolism implies that its loss may weaken antioxidant defenses, heightening oxidative

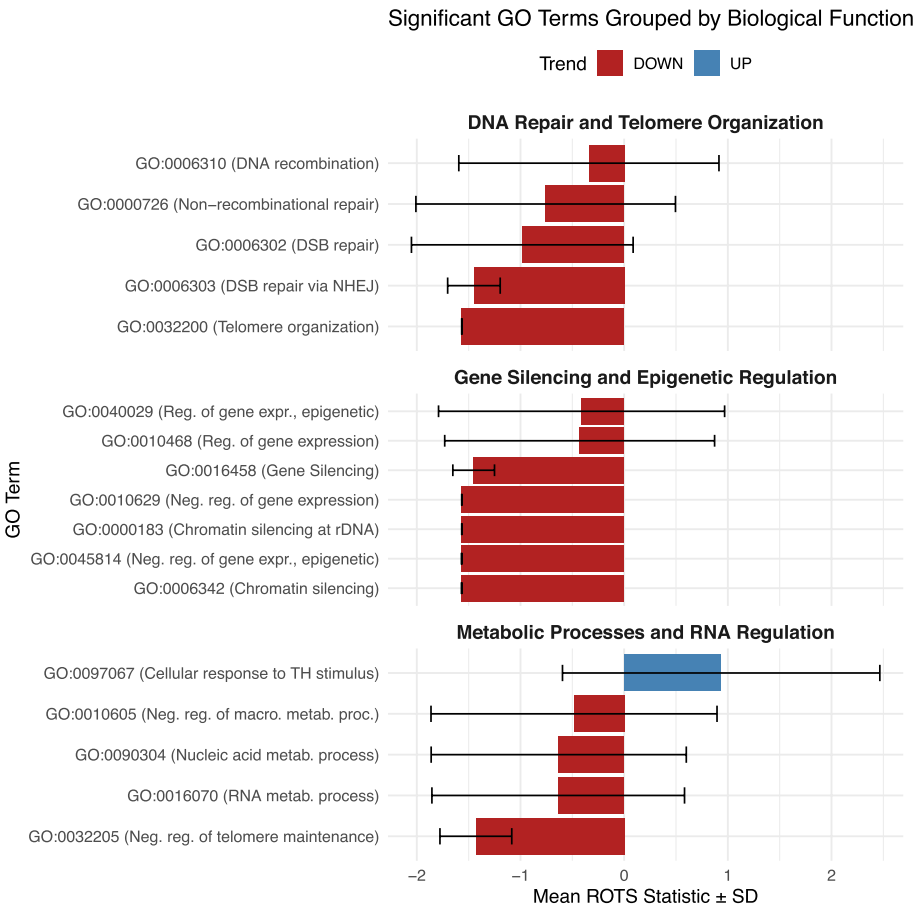

Fig. 3 Significant Gene Ontology (GO) terms grouped by biological function based on ROTS statistics: Each bar represents the mean ROTS statistic for genes annotated under a specific GO term, grouped into three categories: Gene Silencing and Epigenetic Regulation, DNA Repair and Telomere Organization, and Metabolic Processes and RNA Regulation. Bars are colored by trend in expression: UP (blue) for positively regulated GO terms and DOWN (red) for negatively regulated ones in rpAD compared to spAD. Error bars indicate ±1 standard deviation. GO term labels include both the identifier and a descriptive name

stress damage [48]. TPM1 reduction likely destabilizes actin filaments in dendritic spines, accelerating synaptic collapse and cognitive decline [49]. Lowered SPON1 removes an endogenous inhibitor of BACE1 cleavage of APP, potentially driving the Aβ accumulation in rpAD [50]. Increased CSF levels of spondin 1 in the AD compared to normal controls have been noted [51]. An association between the minor allele (A) of rs11023139 in the SPON1 gene and reduced rates of cognitive decline during the later stages of AD has been reported in the Alzheimer's Disease Neuroimaging Initiative (ADNI) study [52]. Additionally, the same locus has been implicated as a factor in cognitive decline during the preclinical stages of AD in the Australian Imaging, Biomarkers and Lifestyle Study of Aging (AIBL) [53]. Older people with SPON1 variant at rs2618516 also had significantly milder clinical dementia scores and lower risk of AD [54].

Reduced CLU and HSPA5 indicate impaired extracellular and ER proteostasis, respectively, critical for protein folding and misfolded protein clearance [55, 56].

SMOC1, a matricellular protein enriched in amyloid plaques in early-onset AD and Down syndrome-associated AD [57], is significantly downregulated in our rpAD cohort. Its reduction may impair extracellular matrix remodeling or limit protective signaling cascades associated with plaque containment and stabilization, potentially facilitating a more permissive environment for neurotoxic Aβ species aggregation.

A2M inhibits Aβ fibril formation and promotes its clearance via LRP1 [58]. When A2M and LRP1 are downregulated in rpAD, they could synergistically impair Aβ clearance. Decreased A2M levels would result in fewer Aβ-A2M complexes, while reduced LRP1 expression would limit the capacity to transport these complexes across the blood-brain barrier.

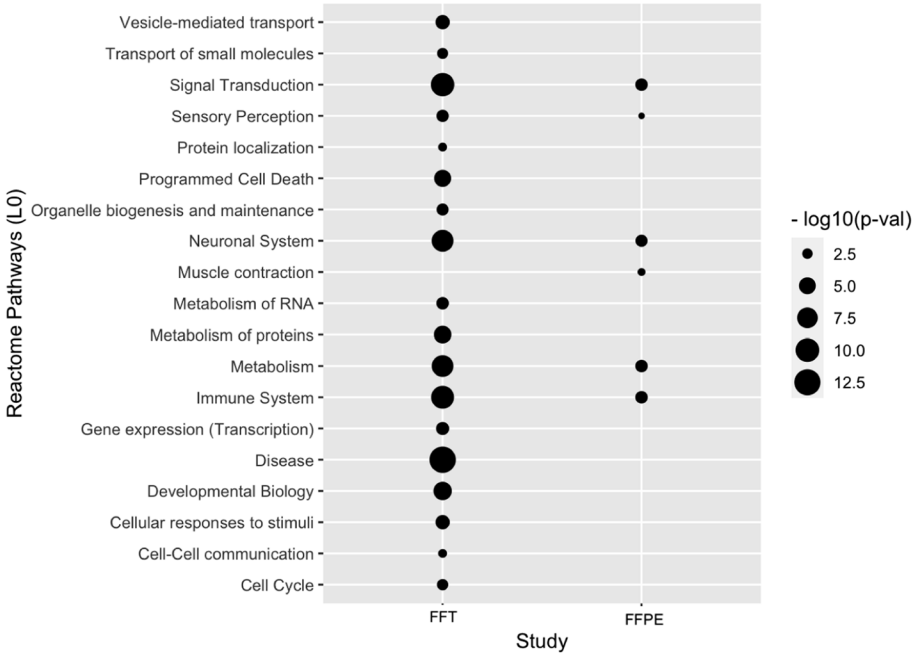

Fig. 4 Pathway enrichment scores are shown for significant pathways identified from FFT and FFPE [15] datasets. The pathways database is collected from the Reactome Pathway Database, where only top-level pathways are considered. While there is an overlap in identified pathways, there are more annotations identified in our study

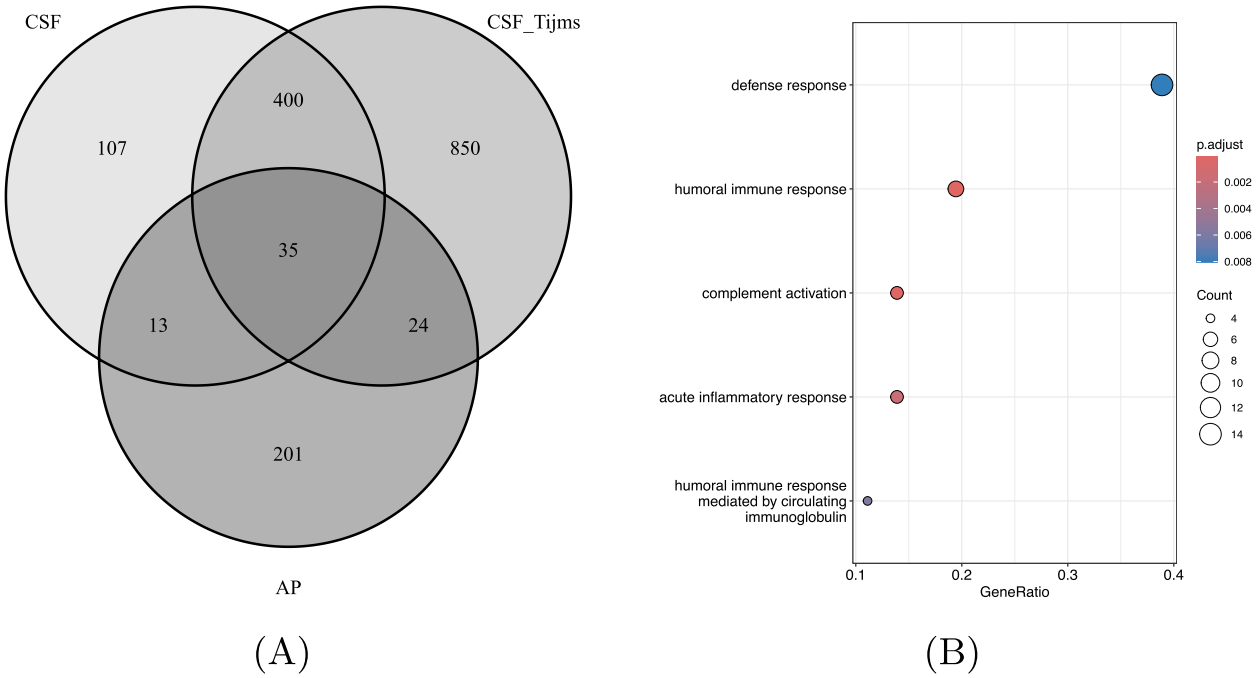

Fig. 5 **A** This Venn diagram illustrates the overlap and differences in protein expression between cerebrospinal fluid (CSF) samples from the rapid subtype from [25], rpAD Amyloid Plaque FFT (AP), and rpAD CSF samples. The overlapping region indicates that 35 proteins are significantly altered in AP (amyloid plaque) samples and observed in CSF samples. **B** The dot plot visualizes the enrichment of biological processes within these 35 proteins. The y-axis lists the enriched processes, while the x-axis represents the GeneRatio, indicating the proportion of genes within the set associated with each process. The size of the dots corresponds to the number of genes involved in each process, and the color represents the statistical significance of the enrichment (lower p-values indicated by warmer colors)

Haptoglobin (HP), an apolipoprotein E (APOE) antioxidant, binds APOE and Aβ, facilitating its clearance, as previously reported [59]. NRXN1, a key synaptic adhesion molecule reduced in rpAD, indicating impaired synaptic integrity [60]; and CTSB/CTSH, lysosomal enzymes whose decline may impede proteolytic clearance of toxic aggregates. Downregulation of NID2, LAMB1, and FBLN1, all ECM structural genes, underscores loss of matrix integrity and vascular support, while suppression of C3, CD55, and SERPINA3 reveals broad immune and complement dysfunction—potentially leading to inefficient clearance and increased vulnerability to inflammatory damage [38, 61].

Coordinated proteomic downregulation parallels reduced CSF tau in rpAD

Principal component analysis of the 35-protein signature yielded a first component (PC1) that separates rpAD from spAD cases. Spearman's correlation shows that PC1 is inversely associated with MAPT ($\rho = -0.62$, $p < 0.048$), supporting the interpretation that samples exhibiting the greatest coordinated down-regulation of these proteins tend to have the lowest tau levels. By contrast, the relationship between PC1 and NEFL is also negative but does not reach significance ($\rho = -0.44$, $p = 0.18$), indicating that this proteomic axis tracks more closely with tau reduction than with axonal-injury marker variation.

Discussion

This study compared proteins in rpAD using two methods, FFT and FFPE tissue analysis. Despite different tissue preparation methods, we identified overlapping protein coverage, including proteins associated with the immune and nervous systems (Fig. 4). However, the methods also revealed differences. The FFT samples yielded a significantly larger number of proteins not identified as differentially expressed in the FFPE analysis. This list of unique proteins in FFT included many AD-related genes, and GO analysis provided novel biological function differences. Using FFT samples also provided a more precise disease ontology mapping. FFT tissue preparation significantly enhanced our proteomic insights and is interesting for follow up in future analyses. Our analysis identified three main biological themes separating rpAD from spAD.

- Gene Silencing and Epigenetic Regulation: Epigenetic modifications, like DNA methylation and histone modifications, regulate gene expression, leading to activation or silencing and impacting various cellular processes, have been postulated in AD pathophysiology [62]. Most differentially methylated positions in neuropathological 'bulk' cortical tissue are thought to reflect DNA methylation differences occurring in non-neuronal cells [63].
- Metabolic Processes and RNA Regulation: Epigenetic modifications affect post-transcriptional RNA processing, and RNA modifications reciprocally regulate gene expression transcriptionally by influencing the epigenome [64].
- DNA Repair and Telomere Organization: DNA repair mechanisms are crucial for maintaining genome stability. DNA double-strand breaks are among the most serious types of DNA damage, and their signaling and repair are critical [65]. Telomeres are the genomic portions at the ends of linear chromosomes. Telomeric DNA in vertebrates protects them from being recognized as DNA damage that triggers a DNA damage response [66].

Proteomic profiling of eight rpAD and three spAD cases revealed a clear dichotomy among proteins that are altered in rpAD relative to spAD. Additionally, overlapping proteins in rpAD amyloid plaques and CSF informed our mechanistic model of rapid AD. The rapid progression of rpAD is driven by a distinct molecular signature characterized primarily by a widespread failure of essential cellular maintenance and defense systems, rather than the hyperactivation of specific detrimental pathways often associated with typical spAD [67].

This accelerated trajectory may result from a synergistic collapse across multiple cellular systems, as defined by a unique protein expression signature. Key factors include the catastrophic failure of proteostasis, where impaired chaperoning and reduced clearance/modulation allow toxic species to accumulate rapidly. Additionally, lysosomal dysfunction further hinders aggregate clearance, while compromised inflammatory and immune responses fail to effectively tag debris for clearance or mount a typical inflammatory response.

Accelerated synaptic failure and loss of extracellular matrix integrity in rpAD create an unstable environment. Overwhelmed stress responses and metabolic crises generate damage that antioxidant and chaperone systems cannot effectively neutralize. This synergy of failures, resulting in a distinct molecular subtype, potentially drives the rapid progression of rpAD via a catastrophic, widespread breakdown of cellular maintenance, defense, and structural systems. This systemic collapse leads to rapid decline as the brain's impaired resilience and repair capacity allow toxic conformers or baseline damage processes to proceed unchecked.

Our analysis indicates that the primary axis of variation in CSF proteomic profiles ("Coordinated proteomic downregulation parallels reduced CSF tau in rpAD" section) is significantly associated with MAPT levels, a key

marker of tau pathology in AD. The lack of a significant correlation between shared CSF proteins and NEFL suggests that axonal injury, while relevant, may not be the predominant factor driving the observed proteomic differences between rpAD and spAD cases. This aligns with previous studies highlighting the central role of tau pathology in AD progression [68–72].

This study has some limitations. Firstly, the small sample size in this study is exploratory and needs future validation in larger samples. The limited number of spAD cases reflects the stringent matching criteria employed based on age and post-mortem interval relative to the rare rpAD cohort available from our center during the study period. While obtaining additional spAD cases is generally feasible, securing cases that precisely matched the specific post-mortem characteristics of the available rpAD group proved challenging. Additionally, there is limited data on the severity of AD pathology by Braak stage in spAD cases. The absence of APOE $\epsilon 4$ status data in both rpAD and spAD groups further constrains our analysis. Finally, rpAD and spAD were identified in two distinct autopsy cohorts, which may introduce related biases. Replication in larger cohorts is necessary to validate these findings. Furthermore, this study did not include a direct comparison to non-demented control cases, which limits the ability to discern AD-specific changes from normal aging or other non-AD pathologies.

While our study focused on plaque co-aggregates and broad CSF proteomics, future analyses should directly compare these findings with established AD fluid biomarkers like phosphorylated Tau (pTau), total Tau (tTau), and neurofilament light chain (NfL) levels in the same cohort. Such comparisons would help contextualize the identified proteomic signatures within the known spectrum of AD pathology and progression markers, potentially revealing how plaque-associated changes relate to neurodegeneration and tauopathy severity in rpAD versus spAD.

Conclusion

Shared amyloid plaque-related protein compositions can reliably differentiate rpAD and spAD across two brain tissue preparation methods. Differences in protein signatures related to the innate immune system and cellular transport of small molecules were noted between the two brain tissue preparation methods. A shared protein signature could be identified between CSF and amyloid plaque proteomics enriched for neuroinflammation-related proteins. The results support the notion that rpAD has a distinct biological profile compared to spAD, and altered immune changes could be key markers of these AD subtypes. If confirmed in larger studies, a distinct CSF profile in rpAD could aid in prognostication and AD clinical trial evaluation.

Supplementary Information

The online version contains supplementary material available at https://doi.org/10.1186/s13195-025-01767-x.

Additional file 1. This file contains supplementary tables and figures related to the study. The supplementary materials include: **Table S1:** Pairwise differentially expressed proteins identified using ROTS, with statistical significance and FDR-adjusted p-values. **Table S2:** Enriched Gene Ontology (GO) terms associated with differentially expressed proteins. **Figures S1-S8:** Figures illustrating protein expression profiles, gene ontology terms, Venn diagrams, and enrichment of disease ontology categories.

Additional file 2. Proteome Analysis of Amyloid Plaque from FFT samples: This file contains the proteomic data of rpAD and spAD amyloid plaque samples. The data includes log2 LFQ intensity values for various proteins across multiple replicates and additional information such as peptide counts, sequence coverage, molecular weight, and protein identifiers.

Additional file 3. Proteome Analysis of Cerebrospinal Fluid (CSF): This file contains the proteomic data of rpAD cerebrospinal fluid (CSF) samples. The data includes log2 LFQ intensity values for various proteins across multiple replicates and additional information such as peptide counts, sequence coverage, molecular weight, and protein identifiers.

Acknowledgements

We thank the National Prion Disease Pathology Surveillance Center (NPDPSC) for their support and collaboration.

Authors'contributions

J.P. conceptualized the study and wrote the main manuscript text. G.B. completed the bioinformatics analysis and wrote the main manuscript text. M.M. completed proteomic analysis. X.W. completed amyloid plaque preparation. All authors reviewed the manuscript.

Funding

Research funding from the National Institutes of Health P30AG072959, R21A G074287, Centers for Disease Control and Prevention, CJD Foundation, Ionis, Alector, Aging Mind Foundation, Amprion, GE Healthcare, Lewy Body Dementia Association, Michael J Fox Foundation, Alzheimer's Association, Department of Defense, Annabelle Foundation, and Keep Memory Alive Foundation.

Data availability

Data is provided within supplementary information files.

Declarations

Ethical approval and consent to participate

All procedures were performed under protocols approved by the Institutional Review Board at Case Western Reserve University. All patients' data and samples were coded and handled according to NIH guidelines to protect patients' identities.

Consent for publication

Not applicable.

Competing interests

James B Leverenz received research funding from the National Institutes of Health, GE Healthcare, and the Lewy Body Dementia Association, Alzheimer's Association, Jane and Lee Seidman Endowed Chair for Advanced Neurological Education, Cleveland Clinic, Douglas Herthel DVM Memorial Fund. Jagan A Pillai received research funding from the National Institutes of Health, Department of Defense, Annabelle foundation, Keep Memory Alive foundation and the Iverson Family Endowed Chair for Alzheimer's Disease Research. The other co-authors declare no competing interests.

Author details

[1]Center for Proteomics and Bioinformatics, Department of Nutrition, Department of Computer and Data Sciences, Case Western Reserve University, Cleveland 44106, OH, USA. [2]Department of Pharmacology, Case Western Reserve

University, Cleveland 44106, OH, USA. [3]Department of Pathology, University of Arizona, Tucson 85721, AZ, USA. [4]Department of Neurology, National Prion Disease Pathology Surveillance Center, University Hospitals Cleveland Medical Center, Cleveland 44195, OH, USA. [5]Lou Ruvo Center for Brain Health, Neurological Institute, Department of Neurology, Cleveland, OH, USA.

Received: 11 February 2025 Accepted: 16 May 2025
Published online: 27 May 2025

References

1. Group GBDNDC. Global, regional, and national burden of neurological disorders during 1990-2015: a systematic analysis for the Global Burden of Disease Study 2015. Lancet Neurol. 2017;16(11):877–897. https://doi.org/10.1016/S1474-4422(17)30299-5.
2. Wu YT, Beiser AS, Breteler MMB, Fratiglioni L, Helmer C, Hendrie HC, et al. The changing prevalence and incidence of dementia over time - current evidence. Nat Rev Neurol. 2017;13(6):327–39. https://doi.org/10.1038/nrneurol.2017.63.
3. Jellinger KA. Neuropathological assessment of the Alzheimer spectrum. J Neural Transm (Vienna). 2020;127(9):1229–56. https://doi.org/10.1007/s00702-020-02232-9.
4. Cummings JL. Cognitive and behavioral heterogeneity in Alzheimer's disease: seeking the neurobiological basis. Neurobiol Aging. 2000;21(6):845–61. https://doi.org/10.1016/s0197-4580(00)00183-4.
5. Wilkosz PA, Seltman HJ, Devlin B, Weamer EA, Lopez OL, DeKosky ST, et al. Trajectories of cognitive decline in Alzheimer's disease. Int Psychogeriatr. 2010;22(2):281–90. https://doi.org/10.1017/S1041610209991001.
6. Pillai JA, Appleby BS, Safar J, Leverenz JB. Rapidly Progressive Alzheimer's Disease in Two Distinct Autopsy Cohorts. J Alzheimers Dis. 2018;64(3):973–80. https://doi.org/10.3233/JAD-180155.
7. Farlow MR, Small GW, Quarg P, Krause A. Efficacy of rivastigmine in Alzheimer's disease patients with rapid disease progression: results of a meta-analysis. Dement Geriatr Cogn Disord. 2005;20(2–3):192–7. https://doi.org/10.1159/000087301.
8. Wallin AK, Hansson O, Blennow K, Londos E, Minthon L. Can CSF biomarkers or pre-treatment progression rate predict response to cholinesterase inhibitor treatment in Alzheimer's disease? Int J Geriatr Psychiatry. 2009;24(6):638–47. https://doi.org/10.1002/gps.2195.
9. Pillai JA, Cummings JL. Clinical trials in predementia stages of Alzheimer disease. Med Clin North Am. 2013;97(3):439–57. https://doi.org/10.1016/j.mcna.2013.01.002.
10. Livingston G, Huntley J, Liu KY, Costafreda SG, Selbæk G, Alladi S, et al. Dementia prevention, intervention, and care: 2024 report of the Lancet standing Commission. Lancet. 2024;404(10452):572–628. https://doi.org/10.1016/S0140-6736(24)01296-0.
11. Schmidt C, Redyk K, Meissner B, Krack L, von Ahsen N, Roeber S, et al. Clinical features of rapidly progressive Alzheimer's disease. Dement Geriatr Cogn Disord. 2010;29(4):371–8. https://doi.org/10.1159/000278692.
12. Abu-Rumeileh S, Capellari S, Parchi P. Rapidly Progressive Alzheimer's Disease: Contributions to Clinical-Pathological Definition and Diagnosis. J Alzheimers Dis. 2018;63(3):887–97. https://doi.org/10.3233/JAD-171181.
13. Kim C, Haldiman T, Kang SG, Hromadkova L, Han ZZ, Chen W, et al. Distinct populations of highly potent TAU seed conformers in rapidly progressing Alzheimer's disease. Sci Transl Med. 2022;14(626):eabg0253. https://doi.org/10.1126/scitranslmed.abg0253.
14. Cohen ML, Kim C, Haldiman T, ElHag M, Mehndiratta P, Pichet T, et al. Rapidly progressive Alzheimer's disease features distinct structures of amyloid-beta. Brain. 2015;138(Pt 4):1009–22. https://doi.org/10.1093/brain/awv006.
15. Drummond E, Nayak S, Faustin A, Pires G, Hickman RA, Askenazi M, et al. Proteomic differences in amyloid plaques in rapidly progressive and sporadic Alzheimer's disease. Acta Neuropathol. 2017;133(6):933–54. https://doi.org/10.1007/s00401-017-1691-0.
16. Podlesniy P, Llorens F, Puigros M, Serra N, Sepulveda-Falla D, Schmidt C, et al. Cerebrospinal Fluid Mitochondrial DNA in Rapid and Slow Progressive Forms of Alzheimer's Disease. Int J Mol Sci. 2020;21(17). https://doi.org/10.3390/ijms21176298.
17. Noor A, Zafar S, Shafiq M, Younas N, Siegert A, Mann FA, et al. Molecular Profiles of Amyloid-beta Proteoforms in Typical and Rapidly Progressive Alzheimer's Disease. Mol Neurobiol. 2022;59(1):17–34. https://doi.org/10.1007/s12035-021-02566-9.
18. Hyman BT, Trojanowski JQ. Consensus recommendations for the postmortem diagnosis of Alzheimer disease from the National Institute on Aging and the Reagan Institute Working Group on diagnostic criteria for the neuropathological assessment of Alzheimer disease. J Neuropathol Exp Neurol. 1997;56(10):1095–7. https://doi.org/10.1097/00005072-199710000-00002.
19. Yan T, Liang J, Gao J, Wang L, Fujioka H, Alzheimer Disease Neuroimaging I, et al. FAM222A encodes a protein which accumulates in plaques in Alzheimer's disease. Nat Commun. 2020;11(1):411. https://doi.org/10.1038/s41467-019-13962-0.
20. Shevchenko A, Tomas H, Havlis J, Olsen JV, Mann M. In-gel digestion for mass spectrometric characterization of proteins and proteomes. Nat Protoc. 2006;1(6):2856–60. https://doi.org/10.1038/nprot.2006.468.
21. Cox J, Mann M. MaxQuant enables high peptide identification rates, individualized p.p.b.-range mass accuracies and proteome-wide protein quantification. Nat Biotechnol. 2008;26(12):1367–72. https://doi.org/10.1038/nbt.1511.
22. Cox J, Neuhauser N, Michalski A, Scheltema RA, Olsen JV, Mann M. Andromeda: a peptide search engine integrated into the MaxQuant environment. J Proteome Res. 2011;10(4):1794–805. https://doi.org/10.1021/pr101065j.
23. Tyanova S, Temu T, Sinitcyn P, Carlson A, Hein MY, Geiger T, et al. The Perseus computational platform for comprehensive analysis of (prote)omics data. Nat Methods. 2016;13(9):731–40. https://doi.org/10.1038/nmeth.3901.
24. Dazard JE, Xu H, Rao JS. R package MVR for Joint Adaptive Mean-Variance Regularization and Variance Stabilization. Proc Am Stat Assoc. 2011;2011:3849–63.
25. Tijms BM, Vromen EM, Mjaavatten O, Holstege H, Reus LM, van der Lee S, et al. Cerebrospinal fluid proteomics in patients with Alzheimer's disease reveals five molecular subtypes with distinct genetic risk profiles. Nat Aging. 2024;4(1):33–47. https://doi.org/10.1038/s43587-023-00550-7.
26. Milacic M, Beavers D, Conley P, Gong C, Gillespie M, Griss J, et al. The Reactome Pathway Knowledgebase 2024. Nucleic Acids Res. 2024;52(D1):D672–8. https://doi.org/10.1093/nar/gkad1025.
27. Suomi T, Seyednasrollah F, Jaakkola MK, Faux T, Elo LL. ROTS: An R package for reproducibility-optimized statistical testing. PLoS Comput Biol. 2017;13(5):e1005562. https://doi.org/10.1371/journal.pcbi.1005562.
28. Allen M, Kachadoorian M, Quicksall Z, Zou F, Chai HS, Younkin C, et al. Association of MAPT haplotypes with Alzheimer's disease risk and MAPT brain gene expression levels. Alzheimers Res Ther. 2014;6(4):39. https://doi.org/10.1186/alzrt268.
29. Iqbal K, Liu F, Gong CX, Grundke-Iqbal I. Tau in Alzheimer Disease and Related Tauopathies. Curr Alzheimer Res. 2010;7(8):656–64.
30. Karch CM, Goate AM. Alzheimer's Disease Risk Genes and Mechanisms of Disease Pathogenesis. Biol Psychiatry. 2015;77(1):43–51. https://doi.org/10.1016/j.biopsych.2014.05.006.
31. Schellenberg GD, Montine TJ. The Genetics and Neuropathology of Alzheimer's Disease. Acta Neuropathol. 2012;124(3):305–23. https://doi.org/10.1007/s00401-012-0996-2.
32. Oh HSH, Urey DY, Karlsson L, Zhu Z, Shen Y, Farinas A, et al. A cerebrospinal fluid synaptic protein biomarker for prediction of cognitive resilience versus decline in Alzheimer's disease. Nat Med. 2025. https://doi.org/10.1038/s41591-025-03565-2.
33. Skou LD, Johansen SK, Okarmus J, Meyer M. Pathogenesis of DJ-1/PARK7-Mediated Parkinson's Disease. Cells. 2024;13(4):296. https://doi.org/10.3390/cells13040296.
34. Foster EM, Dangla-Valls A, Lovestone S, Ribe EM, Buckley NJ. Clusterin in Alzheimer's Disease: Mechanisms, Genetics, and Lessons From Other Pathologies. Front Neurosci. 2019;13:164. https://doi.org/10.3389/fnins.2019.00164.

35. Fareed MM, Qasmi M, Aziz S, Völker E, Förster CY, Shityakov S. The Role of Clusterin Transporter in the Pathogenesis of Alzheimer's Disease at the Blood-Brain Barrier Interface: A Systematic Review. Biomolecules. 2022;12(10):1452. https://doi.org/10.3390/biom12101452.
36. Liu Z, Dai X, Tao W, et al. APOE Influences Working Memory in Non-Demented Elderly Through an Interaction With SPON1 Rs2618516. Human Brain Mapping. 2018;39(7):2859–67. https://doi.org/10.1002/hbm.24045.
37. Muffat J, Walker DW. Apolipoprotein D: an overview of its role in aging and age-related diseases. Cell Cycle. 2010;9(2):269–73. https://doi.org/10.4161/cc.9.2.10433.
38. Shi Q, Chowdhury S, Ma R, Le KX, Hong S, Caldarone BJ, et al. Complement C3 Deficiency Protects Against Neurodegeneration in Aged Plaque-Rich APP/PS1 Mice. Sci Transl Med. 2017;9(392):eaaf6295. https://doi.org/10.1126/scitranslmed.aaf6295.
39. Martinez-Mir A, González-Pérez A, Gayán J, Antúnez C, Marín J, Boada M, et al. Genetic study of neurexin and neuroligin genes in Alzheimer's disease. J Alzheimers Dis. 2013;35(2):403–12. https://doi.org/10.3233/JAD-122257.
40. Cermak S, Kosicek M, Mladenovic-Djordjevic A, Smiljanic K, Kanazir S, Hecimovic S. Loss of Cathepsin B and L Leads to Lysosomal Dysfunction, NPC-Like Cholesterol Sequestration and Accumulation of the Key Alzheimer's Proteins. PLoS ONE. 2016;11(11):e0167428. https://doi.org/10.1371/journal.pone.0167428.
41. Li R, Zhang J, Wang Q, Cheng M, Lin B. TPM1 mediates inflammation downstream of TREM2 via the PKA/CREB signaling pathway. J Neuroinflammation. 2022;19(1):257. https://doi.org/10.1186/s12974-022-02619-3.
42. Ewers M, Franzmeier N, Suárez-Calvet M, Morenas-Rodriguez E, Caballero MAA, Kleinberger G, et al. Increased soluble TREM2 in cerebrospinal fluid is associated with reduced cognitive and clinical decline in Alzheimer's disease. Sci Transl Med. 2019;11(507):eaav6221. https://doi.org/10.1126/scitranslmed.aav6221.
43. Pillai JA, Khrestian M, Bena J, Leverenz JB, Bekris LM. Temporal Ordering of Inflammatory Analytes sTNFR2 and sTREM2 in Relation to Alzheimer's Disease Biomarkers and Clinical Outcomes. Front Aging Neurosci. 2021;13:676744. https://doi.org/10.3389/fnagi.2021.676744.
44. Liu PP, Liu XH, Ren MJ, Liu XT, Shi XQ, Li ML, et al. Neuronal cathepsin S increases neuroinflammation and causes cognitive decline via CX3CL1-CX3CR1 axis and JAK2-STAT3 pathway in aging and Alzheimer's disease. Aging Cell. 2025;24(2):e14393. https://doi.org/10.1111/acel.14393.
45. Lee HW, Chen SJ, Tsai KJ, Hsu KS, Chen YF, Chang CH, et al. Targeting cathepsin S promotes activation of OLF1-BDNF/TrkB axis to enhance cognitive function. J Biomed Sci. 2024;31:46. https://doi.org/10.1186/s12929-024-01037-2.
46. Castanho I, Murray TK, Hannon E, et al. Transcriptional Signatures of Tau and Amyloid Neuropathology. Cell Rep. 2020;30(6):2040-2054.e5. https://doi.org/10.1016/j.celrep.2020.01.063.
47. Rawat P, Sehar U, Bisht J, et al. Phosphorylated Tau in Alzheimer's Disease and Other Tauopathies. Int J Mol Sci. 2022;23(21):12841. https://doi.org/10.3390/ijms232112841.
48. He Z, Sun X, Wang S, Bai D, Zhao X, Han Y, et al. Ggct plays an important role in erythrocyte antioxidant defense and red blood cell survival. Br J Haematol. 2021. https://doi.org/10.1111/bjh.17775.
49. Pelucchi S, Stringhi R, Marcello E. Dendritic Spines in Alzheimer's Disease: How the Actin Cytoskeleton Contributes to Synaptic Failure. Int J Mol Sci. 2020;21(3):908. https://doi.org/10.3390/ijms21030908.
50. Park SY, Kang JY, Lee T, Nam D, Jeon CJ, Kim JB. SPON1 Can Reduce Amyloid Beta and Reverse Cognitive Impairment and Memory Dysfunction in Alzheimer's Disease Mouse Model. Cells. 2020;9(5):1275. https://doi.org/10.3390/cells9051275.
51. Zhang J, Goodlett DR, Quinn JF, Peskind E, Kaye JA, Zhou Y, et al. Quantitative proteomics of cerebrospinal fluid from patients with Alzheimer disease. J Alzheimers Dis. 2005;7(2):125–33; discussion 173–80. https://doi.org/10.3233/jad-2005-7205.
52. Sherva R, Tripodis Y, Bennett DA, Chibnik LB, Crane PK, de Jager PL, et al. Genome-wide association study of the rate of cognitive decline in Alzheimer's disease. Alzheimers Dement. 2014;10(1):45–52. https://doi.org/10.1016/j.jalz.2013.01.008.
53. Fernandez S, Burnham SC, Milicic L, Savage G, Maruff P, Peretti M, et al. SPON1 Is Associated with Amyloid-β and APOE ϵ4-Related Cognitive Decline in Cognitively Normal Adults. J Alzheimers Dis Rep. 2021;5(1):111–20. https://doi.org/10.3233/ADR-200246.
54. Jahanshad N, Rajagopalan P, Hua X, Hibar DP, Nir TM, Toga AW, et al. Genome-wide scan of healthy human connectome discovers SPON1 gene variant influencing dementia severity. Proc Natl Acad Sci U S A. 2013;110(12):4768–73. https://doi.org/10.1073/pnas.1216206110.
55. Ajoolabady A, Lindholm D, Ren J, Kroemer G, Klionsky DJ, Uversky VN, et al. ER stress and UPR in Alzheimer's disease: mechanisms, pathogenesis, treatments. Cell Death Dis. 2022;13(7):706. https://doi.org/10.1038/s41419-022-05153-5.
56. Foster EM, Dangla-Valls P, Hynänen L, Serrano-Pozo A, Stevens GR, Leskovjan VV, et al. Clusterin in Alzheimer's disease: mechanisms, relevance, and opportunities. CNS Neurosci Ther. 2019;25(9):937–51. https://doi.org/10.1111/cns.13197.
57. Drummond E, Kavanagh T, Pires G, Marta-Ariza M, Kanshin E, Nayak S, et al. The amyloid plaque proteome in early onset Alzheimer's disease and Down syndrome. Acta Neuropathol Commun. 2022;10(1):53. https://doi.org/10.1186/s40478-022-01356-1.
58. Hope C, Mettenburg J, Gonias SL, DeKosky ST, Kamboh MI, Chu CT. Functional analysis of plasma α2-macroglobulin from Alzheimer's disease patients with the A2M intronic deletion. Neurobiol Dis. 2003;14(3):504–12. https://doi.org/10.1016/j.nbd.2003.08.005.
59. Bai H, Naj AC, Benchek P, Dumitrescu L, Hohman T, Hamilton-Nelson K, et al. A haptoglobin (HP) structural variant alters the effect of APOE alleles on Alzheimer's disease. Alzheimers Dement. 2023;19(11):4886–95. https://doi.org/10.1002/alz.13050.
60. Medina-Samamé A, Paller É, Bril MR, Archvadze A, Simões-Abade MBC, Estañol-Cayuela P, et al. Role of Neurexins in Alzheimer's Disease. J Neurosci. 2023;43(23):4194–6. https://doi.org/10.1523/JNEUROSCI.0169-23.2023.
61. Zattoni M, Mearelli M, Vanni S, Colini Baldeschi A, Tran TH, Ferracin C, et al. Serpin Signatures in Prion and Alzheimer's Diseases. Mol Neurobiol. 2022;59(6):3778–99. https://doi.org/10.1007/s12035-022-02817-3.
62. Qazi TJ, Quan Z, Mir A, Qing H. Epigenetics in Alzheimer's disease: perspective of DNA methylation. Mol Neurobiol. 2018;55(2):1026–44. https://doi.org/10.1007/s12035-016-0357-6.
63. Shireby G, Dempster EL, Policicchio S, Smith RG, Pishva E, Chioza B, et al. DNA methylation signatures of Alzheimer's disease neuropathology in the cortex are primarily driven by variation in non-neuronal cell-types. Nat Commun. 2022;13(1):5620. https://doi.org/10.1038/s41467-022-33394-7.
64. Patrasso EA, Raikundalia S, Arango D. Regulation of the epigenome through RNA modifications. Chromosoma. 2023;132(3):231–46. https://doi.org/10.1007/s00412-023-00794-7.
65. Bohgaki T, Bohgaki M, Hakem R. DNA double-strand break signaling and human disorders. Genome Integr. 2010;1(1):15. https://doi.org/10.1186/2041-9414-1-15.
66. Rossiello F, Jurk D, Passos JF, d'Adda di Fagagna F. Telomere dysfunction in ageing and age-related diseases. Nat Cell Biol. 2022;24(2):135–147. https://doi.org/10.1038/s41556-022-00842-x.
67. Targa Dias Anastacio H, Matosin N, Ooi L. Neuronal hyperexcitability in Alzheimer's disease: what are the drivers behind this aberrant phenotype? Transl Psychiatry. 2022;12(1):257. https://doi.org/10.1038/s41398-022-02024-7.
68. Bader JM, Geyer PE, Müller JB, Strauss MT, Koch M, Leypoldt F, et al. Proteome profiling in cerebrospinal fluid reveals novel biomarkers of Alzheimer's disease. Mol Syst Biol. 2020;16(6):e9356. https://doi.org/10.15252/msb.20199356.
69. Bai B, Vanderwall D, Li Y, Wang X, Poudel S, Wang H, et al. Proteomic landscape of Alzheimer's Disease: novel insights into pathogenesis and biomarker discovery. Mol Neurodegener. 2021;16(1):55. https://doi.org/10.1186/s13024-021-00474-z.
70. Higginbotham L, Ping L, Dammer EB, Duong DM, Zhou M, Gearing M, et al. Integrated proteomics reveals brain-based cerebrospinal fluid biomarkers in asymptomatic and symptomatic Alzheimer's disease. Sci Adv. 2020;6(43):eaaz9360. https://doi.org/10.1126/sciadv.aaz9360.

71. Seifar F, Fox EJ, Shantaraman A, Liu Y, Dammer EB, Modeste E, et al. Large-scale deep proteomic analysis in Alzheimer's disease brain regions across race and ethnicity. Alzheimers Dement. 2024;20(12):8878–97. https://doi.org/10.1002/alz.14360.
72. Vromen EM, Del Campo Milán M, Scheltens P, Teunissen CE, Visser PJ, Tijms BM. CSF proteomic signature predicts progression to Alzheimer's disease dementia. Alzheimers Dement (N Y). 2022;8(1):e12240. https://doi.org/10.1002/trc2.12240.

Publisher's Note